ACS OMEGA

http://pubs.acs.org/journal/acsodf

Article

Thermodynamic Properties of Ternary Systems Containing (LiCl and LiBr) + Propylene Carbonate + Ionic Liquid (1-Alkyl-3-methylimidazolium Thiocyanate)

Behrang Golmohammadi, Hemayat Shekaari,* and Mohammed Taghi Zafarani-Moattar

Cite This: *ACS Omega* 2021, 6, 27874−27887

Read Online

ACCESS | Metrics & More | Article Recommendations | Supporting Information

ABSTRACT: The development of the Li-ion battery Industry in a green way is crucial for human beings' future. Ionic liquids (ILs) are green cosolvents that could be applied in Li-ion battery electrolytes. A thermodynamic study has been carried out for a Li-ion electrolyte (propylene carbonate (PC) + LiCl and LiBr) in the presence of IL 1-alkyl-3-methylimidazolium thiocyanate [RMIM][SCN] (R = butyl, hexyl, and octyl). The studied thermodynamic properties were density, speed of sound, apparent molar volume, and compressibility. The effect of ILs in propylene carbonate (PC) has been investigated under atmospheric pressure at T = (288.15−318.15) K. Also, a microscopic approach using scaled particle theory has been implemented. The solvation effect of lithium halides, LiX (X = Cl^-, Br^-), on the volumetric and compressibility properties of the ILs has been studied at 298.15 K. The results show that [OMIM][SCN] has the strongest interactions with PC in the studied ILs and these interactions are more weakened with the addition of LiBr than LiCl. According to the partial molar compressibility results, the systems containing [OMIM][SCN] could be used under pressure more beneficially than other systems from the thermodynamic aspect of view.

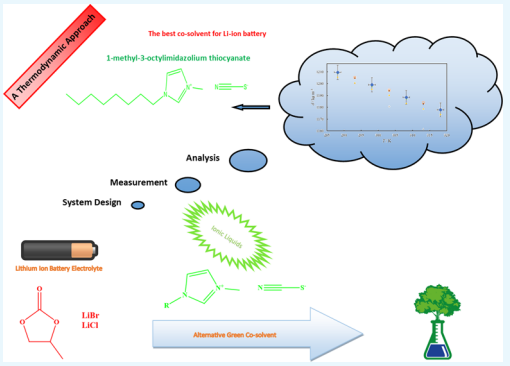

INTRODUCTION

Rechargeable world is the aim of recent research studies to reduce excessive energy resource consumption. Lithium capacitors are one of the most important rechargeable energy-storage devices. The lithium capacitors' industry development led to an increased demand for lithium sources than ever.[1] The investigations about extraction, separation, and purification around the systems containing lithium species have been increased.[2−5] Also, there is some promising investigation that suggests optimization of the capacitors for a long life span instead of expensive separation methods that may cause environmental damages. Achieving environmentally friendly lithium power sources is the subject of the literature.[6−10]

Ionic liquids as environmentally friendly and biodegradable chemicals have advantages for industrial uses such as high thermal stability, etc.[11,12] Imidazole-based ionic liquids with fluorinated anions have been used effectively to enhance the properties of the lithium batteries.[13] However, it found that using fluorinated anion-based ILs may cause environmental damages in long term.[14−16] To overcome this problem, cyano-based anions have been suggested recently. One of the best options for replacing fluorinated anions is thiocyanate.[17,18] The imidazolium-based ILs with a thiocyanate anion are used effectively in various applications. Based on the literature, the use of these ILs, as well as fluorinated ILs, is promising.[19,20]

An electrolyte is an important part of a battery that affects ion mobility and consequently generated energy. Also, the electrolyte is the part that would be eliminated after cycles of usage. Accordingly, the electrolyte is related to the life span of the battery rather than other parts. One of the main and convenient species of a lithium capacitor electrolyte is propylene carbonate (PC) that has the best benefits for the developed technologies of Li capacitors.[21−23] However, there are limited thermodynamic investigations around these systems.

In the present work, in the continuation of our previous experiences, a modeled lithium capacitor electrolyte has been designed to be investigated with a thermodynamic approach.[24,25] The ILs with a thiocyanate anion, [RMIM][SCN] (R = butyl, hexyl, and octyl), have been studied. The density and speed of sound of binary and ternary systems containing (PC + ILs) and (PC + ILs + LiX (X = Cl, Br)), respectively, have been measured. Based on the measured properties, the apparent molar volume and apparent molar isentropic compressibility of the ILs have been evaluated and the standard partial molar volume and partial molar isentropic compressibility have been calculated. Scaled particle theory was used to obtain the different

Received: July 5, 2021
Accepted: September 30, 2021
Published: October 18, 2021

https://doi.org/10.1021/acsomega.1c03517
ACS Omega 2021, 6, 27874−27887

contributions of the standard partial molar volume. The results are used to interpret the interactions between the species.

RESULTS AND DISCUSSION

Volumetric Properties. The density data of propylene carbonate are compared in Figure 1 with the literature and good

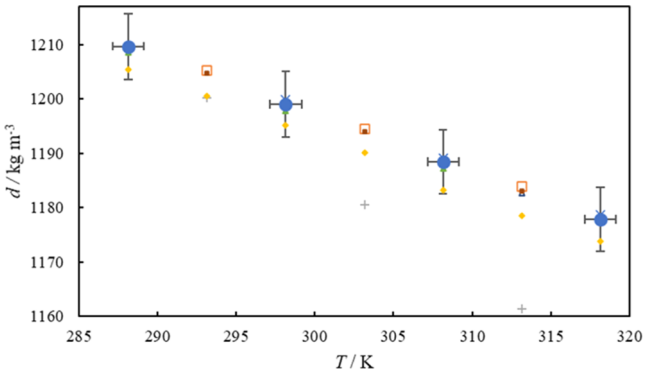

Figure 1. Experimental density of propylene carbonate (PC) versus temperature compared with literature data. Blue multiplication symbol: ref 34, red open square: ref 33, gray plus symbol: ref 32, yellow solid diamond: ref 31, blue solid square: ref 30, green solid triangle: ref 29, blue upward triangle: ref 28, red solid square: ref 27, and blue solid circle: this work.

agreement has been achieved.[27−34] The error bars have been used in a 0.5% range for our data to compare with literature data, which show less difference than this value. However, in the previous work, the density and speed of sound data for propylene carbonate were different due to different sources of the supplier.[25]

The density of solutions containing ([RMIM][SCN] + PC) is measured under atmospheric pressure (P = 0.086 MPa) at temperature ranges T = (288.15−318.15) K. These data are given in Table 1, which shows the density data decrease with the addition of IL content. The apparent molar volumes, V_φ, of the ILs in the PC solutions were evaluated using the following equation[24]

$$V_\varphi = \frac{M}{d} - \left[\frac{(d - d_0)}{m d d_0}\right] \tag{1}$$

where M is the molar mass of the IL, m is the molality of the IL, and d_0 and d are the densities of the solvent (PC) and the solution, respectively. The V_φ values for the studied ILs in binary solutions are given in Table 1, and Figure 2 shows the plot of the V_φ values versus molality of ILs with different cation sizes where the V_φ values increased from butyl to octyl.

Also, the increasing V_φ values with temperature and molality are shown in Figure 3. The standard partial molar volumes, V_φ^0, have been calculated with the Redlich−Mayer equation[24]

$$V_\varphi = V_\varphi^0 + S_v m^{1/2} + B_v m \tag{2}$$

where V_φ^0, S_v, and B_v are given in Table 2, for the binary solutions. The V_φ^0 values are criteria of solute−solvent interaction, while the S_v values are criteria of solute−solute interactions, and B_v is an adjustable parameter. The V_φ^0 values of the studied ILs are increased by the alkyl chain length and increasing temperature in the binary solutions.

Scaled particle theory (SPT), as a microscopic viewpoint, was used to determine different contributions of the partial molar volume, namely, the cavity volume (V_{cav}), the interactional volume (V_{int}), and the state transitional volume ($\kappa_T RT$) changes due to components' isothermal transition from a vapor to liquid phase, and κ_T is isothermal compressibility of the solvent. The corresponding equation is[24,26]

$$V_\varphi^0 = V_{cav} + V_{int} + \kappa_T RT \tag{3}$$

where R is the universal gas constant and T is the absolute temperature. The cavity volume was calculated using equations

$$V_{cav} = \kappa_T RT\left(\frac{y}{1-y} + \frac{3yz(1+z)}{(1-y)^2} + \frac{9y^2z^2}{(1-y)^3}\right) + \frac{\pi\sigma_2^3 N_A}{6} \tag{4}$$

$$y = \frac{\pi N_A \sigma_1^3}{6V} \tag{5}$$

$$z = \frac{\sigma_2}{\sigma_1} \tag{6}$$

In eqs 4−6, N_A is the Avogadro constant, V is the molar volume of the solvent, and σ_1 and σ_2 are the diameters of the solvent (PC) and solute (IL), respectively, which are obtained by a procedure defined by Abraham[35] using the Bondi[36] method for atomic Van der Waals volumes. The symbol z is the ratio of the solute to solvent diameters. The κ_T values for PC were calculated by the following equation

$$\kappa_T = \kappa_S + \frac{\alpha^2 TV}{C_P} \tag{7}$$

where κ_s is isentropic compressibility, C_P is the isobaric heat capacity of the solvent (PC) that is taken from the literature, α is thermal expansion, and V is the molar volume of the solvent. The calculated κ_T values are in good agreement with the literature.[37,38] The calculated values of V_{cav} and V_{int} are given in Table 3. As can be seen, V_{cav} increases and V_{int} decreases with an increase in the alkyl chain length. A more negative value of V_{int} demonstrates stronger solute−solvent interactions between PC and [OMIM][SCN]. However, increasing temperature led to decreased interactions.

The V_φ^0 values of temperature dependency are fitted with a second-degree polynomial equation[24,26]

$$V_\varphi^0 = A + BT + CT^2 \tag{8}$$

where A, B, and C are the empirical parameters of the equation. The standard apparent molar expansibility at constant pressure E_φ^0 was calculated using the following equation[24]

$$E_\varphi^0 = \left(\frac{\partial V_\varphi^0}{\partial T}\right)_p = B + 2CT \tag{9}$$

The E_φ^0 values are given in Table 2. These values are positive and increased with increasing IL cation size. Also, this variable decreased with increasing temperature. The isobaric thermal expansion was evaluated as a function of V_φ^0 and E_φ^0 by the following equation[24]

$$\alpha = \frac{E_\varphi^0}{V_\varphi^0} \tag{10}$$

https://doi.org/10.1021/acsomega.1c03517
ACS Omega 2021, 6, 27874−27887

Table 1. Density (d), Speed of Sound (u), Solvation Number (S_n), Apparent Molar Volume (V_φ), and Apparent Molar Isentropic Compressibility (κ_φ) Data of ([RMIM][SCN] + PC) at T = (288.15 to 318.15) K under Pressure (P = 0.086 MPa)[a]

m_{IL} (mol kg^{-1})	d (kg m^{-3})	u (m s^{-1})	S_n	10^6 V_φ (m^3 mol^{-1})	10^{14} κ_φ (m^3 mol^{-1} Pa^{-1})
			[BMIM][SCN]		
			T = 288.15 K		
0.0000	1209.663	1478.33			
0.0129	1209.398	1479.24	76.49	177.13	4.25
0.0165	1209.324	1479.49	76.27	177.16	4.26
0.0192	1209.268	1479.68	76.24	177.19	4.26
0.0218	1209.214	1479.86	76.06	177.22	4.26
0.0235	1209.179	1479.97	75.59	177.23	4.28
0.0272	1209.103	1480.22	75.29	177.26	4.29
0.0289	1209.066	1480.34	75.24	177.30	4.29
0.0331	1208.978	1480.62	74.80	177.36	4.30
			T = 298.15 K		
0.0000	1199.037	1442.90			
0.0129	1198.772	1443.99	97.46	178.82	3.83
0.0165	1198.697	1444.29	97.19	178.90	3.84
0.0192	1198.641	1444.51	96.61	178.92	3.86
0.0218	1198.587	1444.72	96.12	178.95	3.87
0.0235	1198.551	1444.86	96.03	178.99	3.88
0.0272	1198.475	1445.16	95.74	179.01	3.89
0.0289	1198.437	1445.30	95.50	179.07	3.90
0.0331	1198.349	1445.64	95.20	179.12	3.91
			T = 308.15 K		
0.0000	1188.430	1407.38			
0.0129	1188.172	1408.61	115.65	180.16	3.42
0.0165	1188.100	1408.95	115.52	180.20	3.42
0.0192	1188.045	1409.20	114.93	180.24	3.45
0.0218	1187.992	1409.44	114.50	180.28	3.46
0.0235	1187.957	1409.59	113.91	180.32	3.48
0.0272	1187.883	1409.93	113.65	180.34	3.49
0.0289	1187.847	1410.08	113.03	180.38	3.51
0.0331	1187.761	1410.48	113.41	180.44	3.50
			T = 318.15 K		
0.0000	1177.840	1372.65			
0.0129	1177.595	1373.99	131.76	181.19	3.00
0.0165	1177.527	1374.36	131.60	181.20	3.01
0.0192	1177.475	1374.64	131.52	181.24	3.01
0.0218	1177.425	1374.90	130.90	181.27	3.03
0.0235	1177.392	1375.07	130.62	181.30	3.04
0.0272	1177.322	1375.44	130.20	181.32	3.06
0.0289	1177.288	1375.61	129.80	181.35	3.07
0.0331	1177.207	1376.02	129.02	181.40	3.10
			[HMIM][SCN]		
			T = 288.15 K		
0.0000	1209.663	1478.33			
0.0119	1209.229	1479.24	71.55	211.23	5.70
0.0147	1209.128	1479.44	70.63	211.30	5.73
0.0174	1209.027	1479.64	69.91	211.32	5.75
0.0205	1208.915	1479.87	69.86	211.35	5.75
0.0215	1208.878	1479.94	69.56	211.38	5.76
0.0241	1208.781	1480.13	69.13	211.43	5.78
0.0265	1208.691	1480.30	68.56	211.49	5.80
0.0299	1208.567	1480.54	68.20	211.57	5.81
			T = 298.15 K		
0.0000	1199.037	1442.90			
0.0119	1198.608	1443.98	93.42	213.03	5.34
0.0147	1198.508	1444.22	92.55	213.11	5.37
0.0174	1198.407	1444.46	91.78	213.18	5.40
0.0205	1198.295	1444.74	92.07	213.24	5.39
0.0215	1198.256	1444.83	92.03	213.35	5.39
0.0241	1198.157	1445.04	90.42	213.47	5.45

https://doi.org/10.1021/acsomega.1c03517
ACS Omega 2021, 6, 27874−27887

Table 1. continued

m_{IL} (mol kg^{-1})	d (kg m^{-3})	u (m s^{-1})	S_n	10^6 V_φ (m^3 mol^{-1})	10^{14} κ_φ (m^3 mol^{-1} Pa^{-1})
			T = 298.15 K		
0.0265	1198.066	1445.25	90.11	213.56	5.46
0.0299	1197.941	1445.54	89.80	213.67	5.47
			T = 308.15 K		
0.0000	1188.430	1407.38			
0.0119	1187.999	1408.62	114.74	215.27	4.95
0.0147	1187.898	1408.90	114.12	215.38	4.97
0.0174	1187.796	1409.18	113.48	215.47	4.99
0.0205	1187.683	1409.49	112.93	215.54	5.01
0.0215	1187.644	1409.59	112.70	215.65	5.03
0.0241	1187.545	1409.85	111.97	215.75	5.05
0.0265	1187.453	1410.09	111.47	215.86	5.07
0.0299	1187.327	1410.43	111.37	215.97	5.08
			T = 318.15 K		
0.0000	1177.840	1372.65			
0.0119	1177.409	1374.00	131.25	217.44	4.66
0.0147	1177.308	1374.30	130.09	217.55	4.70
0.0174	1177.206	1374.61	129.88	217.64	4.71
0.0205	1177.092	1374.95	129.40	217.75	4.73
0.0215	1177.055	1375.06	129.29	217.79	4.74
0.0241	1176.956	1375.35	128.86	217.90	4.75
0.0265	1176.865	1375.61	128.21	217.99	4.78
0.0299	1176.740	1375.96	127.11	218.08	4.82
			[OMIM][SCN]		
			T = 288.15 K		
0.0000	1209.683	1478.39			
0.0088	1209.235	1479.26	89.61	244.32	6.37
0.0115	1209.094	1479.50	86.54	244.69	6.48
0.0133	1208.995	1479.66	84.42	244.92	6.56
0.0161	1208.844	1479.88	80.18	245.20	6.70
0.0183	1208.725	1480.04	76.88	245.42	6.81
0.0206	1208.600	1480.21	74.26	245.58	6.90
0.0229	1208.475	1480.35	70.67	245.84	7.03
0.0252	1208.342	1480.50	67.57	246.05	7.13
			T = 298.15 K		
0.0000	1199.037	1442.91			
0.0088	1198.601	1443.94	118.19	245.86	5.81
0.0115	1198.465	1444.23	115.34	246.14	5.91
0.0133	1198.370	1444.43	113.87	246.31	5.97
0.0161	1198.223	1444.70	109.26	246.62	6.13
0.0183	1198.108	1444.90	105.85	246.81	6.26
0.0206	1197.985	1445.11	102.91	247.03	6.36
0.0229	1197.864	1445.29	99.18	247.27	6.50
0.0252	1197.734	1445.49	96.31	247.50	6.61
			T = 308.15 K		
0.0000	1188.430	1407.45			
0.0088	1188.007	1408.60	141.96	247.31	5.31
0.0115	1187.875	1408.93	139.49	247.60	5.41
0.0133	1187.782	1409.15	137.33	247.81	5.50
0.0161	1187.641	1409.48	134.60	248.03	5.60
0.0183	1187.526	1409.71	130.75	248.36	5.75
0.0206	1187.406	1409.95	127.45	248.59	5.88
0.0229	1187.290	1410.18	124.76	248.77	5.98
0.0252	1187.161	1410.41	121.37	249.08	6.12
			T = 318.15 K		
0.0000	1177.840	1372.72			
0.0088	1177.427	1373.98	164.92	249.03	4.76
0.0115	1177.297	1374.34	161.89	249.38	4.89
0.0133	1177.208	1374.59	160.61	249.49	4.94
0.0161	1177.069	1374.95	157.21	249.77	5.09
0.0183	1176.961	1375.23	155.23	249.92	5.17

https://doi.org/10.1021/acsomega.1c03517
ACS Omega 2021, 6, 27874−27887

Table 1. continued

m_{IL} (mol kg^{-1})	d (kg m^{-3})	u (m s^{-1})	S_n	10^6 V_φ (m^3 mol^{-1})	10^{14} κ_φ (m^3 mol^{-1} Pa^{-1})
			T = 318.15 K		
0.0206	1176.845	1375.49	151.09	250.13	5.33
0.0229	1176.732	1375.75	148.37	250.32	5.45
0.0252	1176.606	1376.02	145.36	250.63	5.57

[a]Standard uncertainties for molality, temperature, and pressure were u (m) = 0.002 mol kg^{-1}, u (T) = 0.02 K, and u (P) = 10 hPa, respectively, with a 0.68 level of confidence, and the combined standard uncertainties for density and speed of sound were u_c (d) = 0.07 kg m^{-3} and u_c (u) = 1.3 m s^{-1} with a 0.68 level of confidence. The standard uncertainties for the apparent molar volume and apparent molar isentropic compressibility were u_c (V_φ) = 5.10^{-5} m^3 mol^{-1} (level of confidence of 0.68) and u_c (κ_φ) = 3.10^{-3} m^3 mol^{-1} Pa^{-1} (level of confidence of 0.68), respectively.

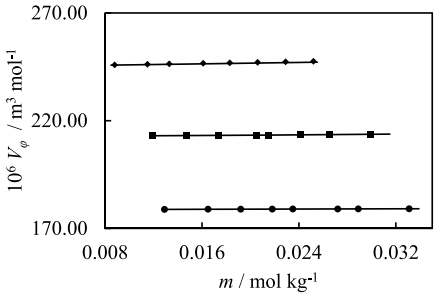

Figure 2. Apparent molar volumes V_φ of [RMIM][SCN] in PC solution versus its molality m at T = 298.15 K. (●) [BMIM][SCN], (■) [HMIM][SCN], and (♦) [OMIM][SCN], and solid lines represent the Redlich−Mayer model.

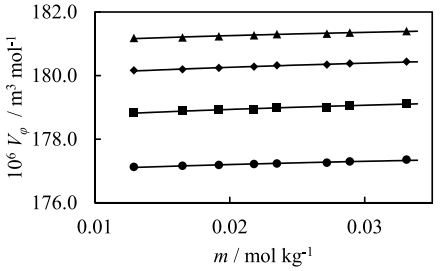

Figure 3. Apparent molar volumes V_φ of [BMIM][SCN] in PC versus its molality m at different temperatures. (●) T = 288.15 K, (■) T = 298.15 K, (♦) T = 308.15 K, and (▲) T = 318.15 K, and solid lines represent the corresponding Redlich−Mayer model.

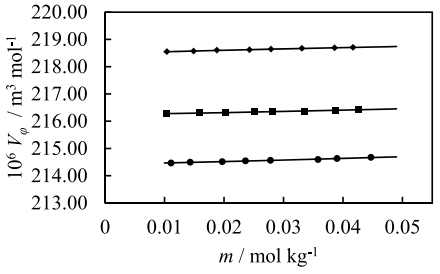

Figure 4. Apparent molar volumes V_φ of [HMIM]SCN against its molality m in a (PC + LiBr) solution at T = 298.15 K at different concentrations of LiBr. (●) 0.0036 mol kg^{-1}, (■) 0.0064 mol kg^{-1}, and (♦) 0.0099 mol kg^{-1}, and solid lines represent the corresponding Redlich−Mayer model.

The calculated values of α for ([RMIM][SCN] + PC) are given in Table 2. The α value is increased with increasing cation size and decreases with increasing temperature. The value of α is a criterion for the response of the volume of a system to increasing temperature. The large value of this factor gets more sensitive in the system volume with temperature change. The

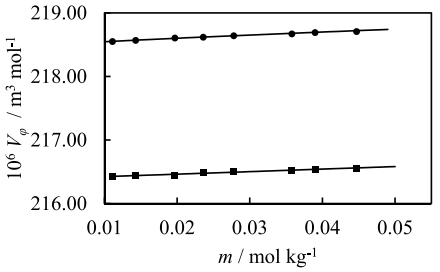

Figure 5. Apparent molar volumes V_φ of [HMIM][SCN] in PC versus its molality m in the presence of about 0.01 mol kg^{-1} of LiX salts at T = 298.15 K. (■) LiCl and (●) LiBr, and solid lines represent the calculated Redlich−Mayer values.

observed trend for α and E_φ^0 is similar to the cavity volume. The pressure would also break the solvent structure and the same reason suggests that the heat capacity decreases. Hepler et al.'s[39] determined relation for structure making or breaking behavior of a solute in a solution is given by the following equations

$$\left(\frac{\partial C_P}{\partial P}\right)_T = -T\left(\frac{\partial^2 V_\varphi^0}{\partial T^2}\right)_P \quad (11)$$

$$-T\left(\frac{\partial^2 V_\varphi^0}{\partial T^2}\right)_P = -2CT \quad (12)$$

where $(\partial^2 V_\varphi{}^0/\partial T^2)$ is the constant for the ILs, as given in Table 2. As can be seen, this parameter decreases with increasing cation size. Negative values of this parameter mean the ILs have structure-breaking behavior in PC, and this behavior intensity order is octyl > hexyl > butyl.The measured density data of ternary solutions containing solute [RMIM][SCN], in the solvent consisting of (PC + LiCl or LiBr), and the corresponding V_φ values that have been calculated with eq 1 are given in Table 4.

The effect of LiX (X = Cl, Br) on the V_φ values of the [HMIM][SCN] is shown in Figure 4. This figure demonstrates that the addition of the LiBr content increases the V_φ values of [HMIM][SCN].

In Figure 5, the effect of anion size (Cl^- and Br^-) on the V_φ values of [HMIM][SCN] has been shown. It is clear that a Br^- anion has a stronger effect rather than a Cl^- anion.

The standard partial molar volumes V_φ^0 of the ILs in (LiX + PC) solutions at different concentrations of LiX are given in Table 5. Results show that a Br^- anion has a stronger effect than a Cl^- anion on the V_φ^0 values. The partial molar volumes of transfer Δ_{tr} V_φ^0 of the ionic liquids have been obtained for [RMIM][SCN] from PC to (LiX + PC) solutions.

https://doi.org/10.1021/acsomega.1c03517
ACS Omega 2021, 6, 27874−27887

Table 2. Standard Partial Molar Volume V_φ^0, Empirical Parameters of eq 2, S_V and B_V, the Standard Deviation of the Apparent Molar Volume $\sigma(V_\varphi)$, Standard Apparent Molar Expansibility E_φ^0, Isobaric Thermal Expansion (α), and the Constant of eq12 $(\partial^2 V_\varphi{}^0/\partial T^2)_p$ for the Solutions of [RMIM][SCN] in PC at Different Temperatures under Pressure (P = 0.086 MPa)[a]

T (K)	$10^6\ V_\varphi{}^0$ ($m^3\ mol^{-1}$)	$10^6\ S_V$ ($m^3\ mol^{-1}\ kg^{-1/2}$)	$10^6\ B_V$ ($m^3\ mol^{-1}\ kg^{-1}$)	$10^6\ \sigma(V_\varphi)$	$10^6\ E_\varphi{}^0$ ($m^3\ mol^{-1}\ K^{-1}$)	$10^4\ \alpha$ (K^{-1})	$10^6\ (\partial^2 V_\varphi{}^0/\partial T^2)$ ($m^3\ mol^{-1}\ K^{-1}$)
			[BMIM][SCN]				
288.15	176.70 ± 0.28	3.81 ± 0.04	−1.92 ± 0.12	0.013	0.1721	9.738	−0.0025
298.15	178.31 ± 0.32	4.67 ± 0.04	−1.71 ± 0.14.	0.015	0.1472	8.253	
308.15	179.64 ± 0.25	4.63 ± 0.03	−1.75 ± 0.11	0.012	0.1222	6.805	
318.15	180.75 ± 0.26	3.87 ± 0.04	−1.99 ± 0.12	0.012	0.0973	5.384	
			[HMIM][SCN]				
288.15	211.57 ± 0.32	−8.12 ± 0.05	46.53 ± 0.16	0.014	0.2313	10.9318	−0.0048
298.15	213.52 ± 0.60	−13.97 ± 0.09	86.42 ± 0.31	0.026	0.1837	8.6029	
308.15	215.31 ± 0.48	−7.54 ± 0.07	66.22 ± 0.24	0.021	0.1361	6.3207	
318.15	216.31 ± 0.17	10.3 ± 0.02	−0.55 ± 0.09	0.014	0.0885	4.0911	
			[OMIM][SCN]				
288.15	241.95 ± 0.14	25.13 ± 0.02	3.35 ± 0.09	0.022	0.2918	12.06	−0.0059
298.15	244.84 ± 0.24	2.44 ± 0.04	90.02 ± 0.15	0.009	0.2327	9.503	
308.15	246.47 ± 0.22	−1.58 ± 0.04	112.58 ± 0.14	0.030	0.1735	7.041	
318.15	248.18 ± 0.26	1.33 ± 0.04	86.74 ± 0.16	0.040	0.1144	4.610	

[a]Standard uncertainties for temperature and pressure were u (T) = 0.02K and u (P) = 10 hPa, respectively, with a 0.68 level of confidence.

Table 3. Isothermal Compressibility (κ_T), Isothermal Volume Transition Contribution ($\kappa_T RT$), and Interactional and Cavity Volumes of the Standard Partial Molar Volume of [RMIM][SCN] in Propylene Carbonate with SPT at T = (288.15−318.15) K under Pressure (P = 0.086 MPa)[a]

T (K)	$10^{10}\ \kappa_T$ (Pa^{-1})	$10^6\ \kappa_T RT$ ($m^3\ mol^{-1}$)	$10^6\ V_{cav}$	$10^6\ V_{int}$
		[BMIM][SCN]		
288.15	5.22	1.25	1563.23	−1391.64
298.15	5.08	1.26	1465.88	−1292.68
308.15	5.00	1.28	1376.51	−1201.98
318.15	4.99	1.32	1294.33	−1118.69
		[HMIM][SCN]		
288.15	5.60	1.34	1760.58	−1567.32
298.15	5.17	1.28	1651.17	−1456.08
308.15	4.90	1.26	1550.73	−1353.96
318.15	4.79	1.24	1458.38	−1260.68
		[OMIM][SCN]		
288.15	5.99	1.44	2015.52	−1778.93
298.15	5.43	1.35	1890.17	−1650.69
308.15	5.05	1.30	1775.11	−1534.00
318.15	4.86	1.28	1669.32	−1426.50

[a]Standard uncertainties for temperature and pressure were u (T) = 0.02K and u (P) = 10 hPa, respectively, with a 0.68 level of confidence.

$$\Delta_{tr} V_\varphi^0 = V_\varphi^0(\text{in PC + LiX(X = Cl, Br)}) - V_\varphi^0(\text{in PC}) \quad (13)$$

The $\Delta_{tr} V_\varphi^0$ values are reported in Table 5. These values are positive and increase with increasing LiX concentration. The $\Delta_{tr} V_\varphi^0$ value is a measure of interaction between solute1 (IL) and solute2 (LiX). The possible interactions for the studied solutions due to the different functional groups of the components are polar−ionic, polar−polar, polar−nonpolar, and nonpolar−nonpolar interactions.[40,41] According to the cosphere overlap model, the positive $\Delta_{tr} V_\varphi^0$ value indicates strong ion−ion and ion−polar interactions between [RMIM]-[SCN] and LiX.[24,26] On the other hand, LiBr has stronger interactions than LiCl with ionic liquids, as shown in Table 5.

Compressibility Properties. The measured speeds of sound (u) data for the binary (IL + PC) and ternary (IL + PC +LiX) solutions are given in Tables 1 and 4, respectively. These data were used to calculate the isentropic compressibility, κ_s, with help of Laplace−Newton's relation.[24]

$$\kappa_s = \frac{1}{du^2} \quad (14)$$

This quantity can be considered as the bulk modulus behavior of the solution. The solvation numbers were calculated from the κ_s values by the Pasynski equation.[42]

$$S_n = \frac{n_1}{n_2}\left(1 - \frac{\kappa_s}{\kappa_{s0}}\right) \quad (15)$$

where n_1 and n_2 are numbers of moles of the solvent and the solute, respectively, and κ_s and κ_{s0} are isentropic compressibility of the solution and the solvent [PC or (PC + LiX)], respectively. The calculated values of S_n are given in Tables 1 and 4 for the investigated binary and ternary solutions. The S_n values were increased with increasing temperature. These values were decreased with the addition of the LiX salt. This may be related to the coordination of PC molecules to Li^+, as confirmed by the Raman spectroscopy study of the lithium salts in PC.[40]

https://doi.org/10.1021/acsomega.1c03517
ACS Omega 2021, 6, 27874−27887

Table 4. Density (d), Speed of Sound (u), Solvation Number (S_n), Apparent Molar Volume (V_φ), and Apparent Molar Compressibility (κ_φ) Data of [RMIM][SCN] in (PC + LiX (X = Cl^- and Br^-)) Solutions at T = 298.15 K under Pressure (P = 0.086 MPa)[a]

m_{IL} (mol kg^{-1})	d (kg m^{-3})	u (m s^{-1})	S_n	10^6 V_φ (m^3 mol^{-1})	10^{14} κ_φ (m^3 mol^{-1} Pa^{-1})
			[BMIm]SCN + PC + LiBr		
			m_{LiBr} = 0.0035 mol kg^{-1}		
0.0000	1199.180	1442.83			
0.0141	1198.884	1443.78	74.26	179.16	4.64
0.0177	1198.808	1444.04	75.53	179.19	4.59
0.0206	1198.748	1444.25	76.50	179.20	4.56
0.0250	1198.656	1444.59	78.46	179.20	4.49
0.0281	1198.591	1444.83	79.53	179.22	4.45
0.0317	1198.515	1445.11	80.39	179.22	4.42
0.0340	1198.467	1445.29	81.02	179.23	4.40
0.0383	1198.375	1445.62	81.54	179.26	4.38
			m_{LiBr} = 0.0062 mol kg^{-1}		
0.0000	1199.383	1442.70			
0.0142	1199.040	1443.60	66.34	181.34	5.00
0.0167	1198.979	1443.77	67.27	181.38	4.97
0.0197	1198.905	1443.98	68.28	181.41	4.93
0.0235	1198.813	1444.24	69.18	181.46	4.90
0.0290	1198.679	1444.63	70.50	181.49	4.85
0.0326	1198.590	1444.90	71.66	181.53	4.81
0.0334	1198.571	1444.98	72.82	181.54	4.77
0.0385	1198.444	1445.35	73.40	181.59	4.75
			m_{LiBr} = 0.0097 mol kg^{-1}		
0.0000	1199.688	1442.63			
0.0131	1199.333	1443.40	57.91	183.40	5.37
0.0172	1199.220	1443.66	59.10	183.42	5.33
0.0189	1199.174	1443.77	59.83	183.46	5.30
0.0242	1199.028	1444.10	60.14	183.48	5.29
0.0282	1198.920	1444.36	61.04	183.49	5.26
0.0325	1198.802	1444.65	62.07	183.52	5.22
0.0358	1198.712	1444.89	63.43	183.55	5.18
0.0392	1198.618	1445.15	64.93	183.58	5.12
			[BMIm]SCN + PC + LiCl		
			m_{LiCl} = 0.0031 mol kg^{-1}		
0.0000	1199.109	1442.84			
0.0138	1198.829	1443.85	83.11	178.70	4.33
0.0171	1198.761	1444.10	83.46	178.71	4.31
0.0211	1198.681	1444.40	84.12	178.72	4.29
0.0241	1198.619	1444.63	84.39	178.74	4.28
0.0295	1198.510	1445.04	84.97	178.77	4.26
0.0332	1198.434	1445.32	85.00	178.78	4.25
0.0359	1198.377	1445.53	85.14	178.82	4.25
0.0395	1198.302	1445.80	85.13	178.86	4.25
			m_{LiCl} = 0.0059 mol kg^{-1}		
0.0000	1199.241	1442.73			
0.0130	1198.960	1443.63	77.12	179.63	4.58
0.0174	1198.864	1443.94	77.31	179.65	4.57
0.0204	1198.798	1444.16	77.88	179.67	4.55
0.0240	1198.721	1444.41	77.96	179.68	4.55
0.0290	1198.611	1444.77	78.22	179.71	4.54
0.0331	1198.523	1445.07	78.75	179.71	4.52
0.0356	1198.467	1445.26	79.09	179.73	4.50
0.0400	1198.372	1445.58	79.41	179.75	4.49
			m_{LiCl} = 0.0100 mol kg^{-1}		
0.0000	1199.447	1442.65			
0.0131	1199.142	1443.47	66.79	180.70	4.99
0.0174	1199.042	1443.74	66.94	180.74	4.98
0.0198	1198.987	1443.89	67.04	180.74	4.98
0.0234	1198.901	1444.13	67.56	180.77	4.96
0.0280	1198.796	1444.42	67.78	180.78	4.95

https://doi.org/10.1021/acsomega.1c03517
ACS Omega 2021, 6, 27874−27887

Table 4. continued

m_{IL} (mol kg^{-1})	d (kg m^{-3})	u (m s^{-1})	S_n	10^6 V_φ (m^3 mol^{-1})	10^{14} κ_φ (m^3 mol^{-1} Pa^{-1})
			m_{LiCl} = 0.0100 mol kg^{-1}		
0.0318	1198.706	1444.66	67.68	180.82	4.95
0.0355	1198.620	1444.91	68.29	180.83	4.93
0.0388	1198.543	1445.12	68.27	180.84	4.93
			[HMIm]SCN + PC + LiBr		
			m_{LiBr} = 0.0035 mol kg^{-1}		
0.0000	1199.208	1442.87			
0.0111	1198.787	1443.58	56.07	214.47	6.67
0.0143	1198.662	1443.80	56.94	214.49	6.64
0.0197	1198.458	1444.15	57.06	214.51	6.64
0.0236	1198.311	1444.41	57.58	214.55	6.62
0.0278	1198.149	1444.70	58.11	214.56	6.60
0.0358	1197.847	1445.25	59.09	214.59	6.56
0.0390	1197.726	1445.46	59.05	214.63	6.56
0.0447	1197.508	1445.85	59.31	214.67	6.55
			m_{LiBr} = 0.0058 mol kg^{-1}		
0.0000	1199.497	1442.76			
0.0103	1199.076	1443.38	48.23	216.27	7.02
0.0159	1198.848	1443.72	48.56	216.31	7.00
0.0203	1198.672	1443.99	49.16	216.32	6.98
0.0251	1198.477	1444.29	49.62	216.34	6.96
0.0282	1198.348	1444.49	49.89	216.35	6.95
0.0336	1198.130	1444.82	49.90	216.36	6.95
0.0387	1197.926	1445.13	49.97	216.40	6.95
0.0426	1197.767	1445.38	50.28	216.43	6.94
			m_{LiBr} = 0.0095 mol kg^{-1}		
0.0000	1199.743	1442.58			
0.0104	1199.284	1443.17	41.01	218.55	7.35
0.0149	1199.085	1443.43	41.35	218.57	7.34
0.0188	1198.916	1443.65	41.47	218.61	7.34
0.0243	1198.673	1443.97	41.72	218.62	7.33
0.0279	1198.515	1444.18	41.94	218.64	7.32
0.0331	1198.287	1444.48	42.02	218.67	7.32
0.0386	1198.046	1444.80	42.17	218.69	7.31
0.0417	1197.911	1444.99	42.58	218.71	7.30
			[HMIm]SCN + PC + LiCl		
			m_{LiCl} = 0.0033 mol kg^{-1}		
0.0000	1199.225	1442.85			
0.0114	1198.793	1443.63	62.35	214.41	6.47
0.0142	1198.686	1443.83	62.96	214.42	6.44
0.0191	1198.501	1444.17	63.16	214.43	6.44
0.0248	1198.285	1444.57	63.42	214.45	6.42
0.0299	1198.093	1444.92	63.32	214.48	6.43
0.0328	1197.980	1445.13	63.45	214.50	6.42
0.0381	1197.781	1445.51	63.93	214.52	6.40
0.0401	1197.705	1445.66	64.31	214.55	6.39
			m_{LiCl} = 0.0061 mol kg^{-1}		
0.0000	1199.368	1442.75			
0.0103	1198.958	1443.40	53.41	215.54	6.82
0.0146	1198.789	1443.68	54.52	215.57	6.78
0.0185	1198.636	1443.93	54.81	215.59	6.77
0.0229	1198.460	1444.22	55.14	215.61	6.76
0.0292	1198.209	1444.63	55.27	215.65	6.76
0.0331	1198.055	1444.89	55.67	215.67	6.74
0.0375	1197.881	1445.17	55.50	215.69	6.75
0.0426	1197.681	1445.51	55.93	215.72	6.73
			m_{LiCl} = 0.0104 mol kg^{-1}		
0.0000	1199.467	1442.62			
0.0111	1199.014	1443.23	42.04	216.43	7.25
0.0143	1198.880	1443.42	42.92	216.44	7.22
0.0197	1198.661	1443.73	43.66	216.45	7.20

https://doi.org/10.1021/acsomega.1c03517
ACS Omega 2021, 6, 27874−27887

Table 4. continued

m_{IL} (mol kg^{-1})	d (kg m^{-3})	u (m s^{-1})	S_n	$10^6\ V_\varphi$ (m^3 mol^{-1})	$10^{14}\ \kappa_\varphi$ (m^3 mol^{-1} Pa^{-1})
			m_{LiCl} = 0.0104 mol kg^{-1}		
0.0236	1198.503	1443.95	43.80	216.48	7.19
0.0278	1198.329	1444.19	43.76	216.50	7.19
0.0358	1198.005	1444.65	44.18	216.52	7.18
0.0390	1197.876	1444.84	44.55	216.54	7.16
0.0447	1197.644	1445.17	44.68	216.56	7.16
			[OMIm]SCN + PC + LiBr		
			m_{LiBr} = 0.0038 mol kg^{-1}		
0.0000	1199.227	1442.80			
0.0096	1198.733	1443.41	44.26	247.20	8.39
0.0133	1198.543	1443.66	45.84	247.26	8.34
0.0155	1198.428	1443.81	46.29	247.27	8.32
0.0184	1198.280	1444.01	47.22	247.30	8.29
0.0237	1198.010	1444.37	48.03	247.33	8.26
0.0266	1197.856	1444.58	48.60	247.37	8.24
0.0300	1197.686	1444.81	48.97	247.37	8.23
0.0322	1197.570	1444.98	49.74	247.39	8.20
			m_{LiBr} = 0.0060 mol kg^{-1}		
0.0000	1199.422	1442.68			
0.0099	1198.897	1443.28	39.14	248.38	8.61
0.0127	1198.743	1443.47	40.65	248.44	8.56
0.0162	1198.562	1443.69	41.38	248.43	8.54
0.0194	1198.389	1443.90	41.82	248.44	8.52
0.0227	1198.217	1444.11	42.20	248.47	8.51
0.0263	1198.027	1444.34	42.41	248.49	8.50
0.0299	1197.832	1444.58	42.76	248.53	8.49
0.0322	1197.709	1444.74	43.32	248.58	8.47
			m_{LiBr} = 0.0098 mol kg^{-1}		
0.0000	1199.584	1442.52			
0.0097	1199.043	1443.09	34.22	250.03	8.85
0.0132	1198.850	1443.31	35.92	250.07	8.79
0.0168	1198.648	1443.54	36.95	250.13	8.76
0.0194	1198.504	1443.70	37.13	250.14	8.75
0.0244	1198.230	1444.02	38.23	250.16	8.71
0.0267	1198.100	1444.18	39.03	250.19	8.68
0.0302	1197.904	1444.40	39.04	250.22	8.68
0.0330	1197.749	1444.59	39.71	250.25	8.66
			[OMIm]SCN + PC + LiCl		
			m_{LiCl} = 0.0032 mol kg^{-1}		
0.0000	1199.177	1442.90			
0.0110	1198.620	1443.65	51.88	246.98	8.13
0.0140	1198.445	1443.89	52.32	247.04	8.11
0.0180	1198.237	1444.18	52.92	247.07	8.09
0.0200	1198.161	1444.29	53.41	247.12	8.07
0.0240	1197.926	1444.62	53.81	247.13	8.06
0.0290	1197.715	1444.91	53.77	247.17	8.06
0.0300	1197.646	1445.01	54.00	247.18	8.05
0.0340	1197.459	1445.29	54.86	247.21	8.02
			m_{LiCl} = 0.0064 mol kg^{-1}		
0.0000	1199.276	1442.74			
0.0100	1198.724	1443.41	44.61	248.42	8.44
0.0150	1198.479	1443.72	45.77	248.49	8.40
0.0170	1198.394	1443.83	46.22	248.51	8.39
0.0200	1198.233	1444.04	46.99	248.55	8.36
0.0220	1198.124	1444.18	47.24	248.58	8.35
0.0260	1197.869	1444.51	47.76	248.60	8.33
0.0300	1197.669	1444.77	48.10	248.62	8.32
0.0320	1197.556	1444.92	48.38	248.63	8.31
			m_{LiCl} = 0.0100 mol kg^{-1}		
0.0000	1199.413	1442.63			
0.0095	1198.887	1443.17	32.51	250.01	8.92

https://doi.org/10.1021/acsomega.1c03517
ACS Omega 2021, 6, 27874−27887

Table 4. continued

m_{IL} (mol kg^{-1})	d (kg m^{-3})	u (m s^{-1})	S_n	10^6 V_φ (m^3 mol^{-1})	10^{14} κ_φ (m^3 mol^{-1} Pa^{-1})
			m_{LiCl} = 0.0100 mol kg^{-1}		
0.0133	1198.675	1443.40	33.78	250.05	8.88
0.0155	1198.551	1443.54	34.70	250.07	8.85
0.0184	1198.391	1443.72	35.53	250.11	8.82
0.0237	1198.100	1444.04	36.04	250.13	8.80
0.0266	1197.934	1444.23	36.63	250.16	8.78
0.0300	1197.750	1444.45	37.56	250.19	8.75
0.0322	1197.625	1444.60	38.11	250.21	8.73

[a]Standard uncertainties for molality, temperature, and pressure were u (m) = 0.002 mol kg^{-1}, u (T) = 0.02 K, and u (P) = 10 hPa, respectively, with a 0.68 level of confidence, and the combined standard uncertainties for density and speed of sound were u_c (d) = 0.07 kg m^{-3} and u_c (u) = 1.3 m s^{-1} with a 0.68 of level of confidence. The standard uncertainties of the apparent molar volume and apparent molar isentropic compressibility were u_c (V_φ) = 5.10^{-5} m^3 mol^{-1} (level of confidence of 0.68) and u_c (κ_φ) = 3.10^{-3} m^3 mol^{-1} Pa^{-1} (level of confidence of 0.68), respectively.

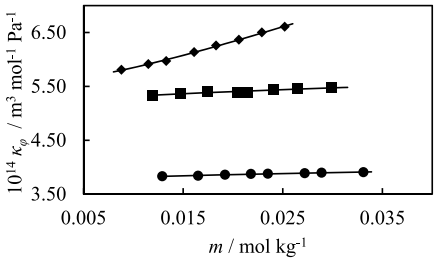

Figure 6. Apparent molar isentropic compressibility κ_φ values of [RMIM][SCN] versus its molality m at T = 298.15 K. (●) [BMIM][SCN], (■) [HMIM][SCN], and (♦) [OMIM][SCN], and solid lines show the corresponding Redlich−Mayer model.

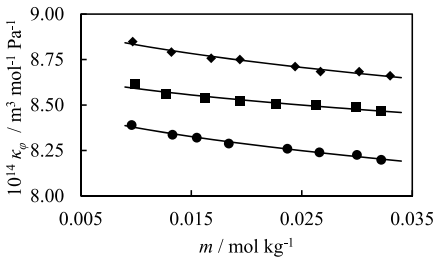

Figure 7. Apparent molar isentropic compressibility values, κ_φ, of [OMIM][SCN] in PC + LiBr {(●) 0.0038 mol kg^{-1}, (■) 0.0060 mol kg^{-1}, and (♦) 0.0092 mol kg^{-1}}, and solid lines show the Redlich model at T = 298.15 K.

Consequently, IL solvation numbers were decreased. It means that the coordination of PC to Li^+ is more favorable rather than the IL solvation.

The apparent molar isentropic compressibility, κ_φ, of the ILs has been determined in the solution with the following relation[24]

$$\kappa_\varphi = \frac{\kappa_S d_0 - d\kappa_{S_0}}{mdd_0} + \frac{\kappa_S M}{d} \quad (16)$$

The κ_φ values of the ILs in the studied solutions are given in Tables 1 and 4 for the corresponding binary and ternary solutions, respectively. These values increase by the addition of the IL in the studied binary solutions (IL + PC). The κ_φ values are higher for a longer alkyl chain length of the ILs [OMIM][SCN], as shown in Figure 6.

The results indicate that the κ_φ values of the ILs, [OMIM][SCN], increase at a higher concentration of LiBr (Figure 7).

Also, it found that the LiBr solution κ_φ values are larger than LiCl solutions, as given in Table 4. The influence of temperature on the κ_φ values of [BMIM][SCN] at (288.15−318.15) K is plotted in Figure 8, which represents a decreasing trend at a higher temperature.

The obtained κ_φ values of the studied ILs of binary (IL + PC) and ternary (IL + LiX + PC) solutions were fitted to the following equation[24]

$$\kappa_\varphi = \kappa_\varphi^0 + S_k m^{1/2} + B_k m \quad (17)$$

where κ_φ^0 is the partial molar isentropic compressibility and S_k and B_k are the empirical parameters of the equation. The obtained parameters for the investigated solutions are listed in Tables 6 and 7 for the studied solutions. The κ_φ^0 values increase with the alkyl chain length of the ILs.

The κ_φ^0 values for the ILs in PC and in the presence of LiX salts are positive, which increase with increasing LiX content, and also, it is found that the value κ_φ^0 in the presence of LiBr is higher than LiCl. This trend shows that bulk propylene carbonate is more compressible rather than electrostrictive PC molecules (solvated PC molecules); upon addition of LiX, electrostriction interactions between IL and PC become weaker due to PC molecules' coordination on Li^+, as previously mentioned. On the other hand, according to the SPT results, it is seen that interactional and cavity volumes are increased for a longer alkyl chain length of the ILs. The highly available cavity volume is the main reason for the high compressibility value of [OMIM]-[SCN] in the PC solution. The intermolecular interaction between the cation of the IL and PC is the dominant factor of this phenomenon but there is intramolecular negative ion interaction, which is another factor that is negligible in the dilute region.

CONCLUSIONS

This study is a thermodynamic approach to a model of Li-ion battery electrolytes. The volumetric and compressibility properties of the ILs, [RMIM][SCN], in PC in the presence of LiCl and LiBr have been investigated to understand the existing interactions in these systems. The ILs' interaction with PC increased with the alkyl chain length of the imidazolium cation from butyl to octyl. However, these interactions were weakened at a higher temperature. The studied ILs, [RMIM][SCN], show structure-breaking behavior in propylene carbonate with the following trend: [OMIM][SCN] > [HMIM][SCN] > [BMIM]-[SCN]. Although ILs with larger cations are more compressible, this feature decreases with increasing temperature. The ion−polar interactions are dominant rather than other interactions in the ternary systems. Also, interactions between LiX and ILs increase with the lithium halide content, and LiBr has a stronger

https://doi.org/10.1021/acsomega.1c03517
ACS Omega 2021, 6, 27874−27887

Table 5. Standard Partial Molar Volume (V_φ^0), Empirical Parameters of eq 2, S_V and B_V, the Partial Molar Volume of Transfer ($\Delta_{tr} V_\varphi^0$), and the Standard Deviation of the Apparent Molar Volume $\sigma(V_\varphi)$ for the Ternary Solutions Containing (IL + LiX + PC) at Different Concentrations of LiX at T = 298.15 K under Pressure (P = 0.086 MPa)[a]

m_{LiX} (mol kg^{-1})	$10^6 V_\varphi^0$(m^3 mol^{-1})	$10^6 S_V$ (m^3 mol^{-1} kg$^{-1/2}$)	$10^6 B_V$ (m^3 mol^{-1} kg^{-1})	$10^6 \Delta_{tr} V_\varphi^0$ (m^3 mol^{-1})	$10^6 \sigma(V_\varphi^0)$
		[BMIM][SCN] + PC + LiBr			
0.0000	178.31 ± 0.32	4.67 ± 0.04	−1.71 ± 0.15		0.015
0.0035	178.96 ± 0.13	2.02 ± 0.02	−2.96 ± 0.05	0.65	0.008
0.0056	180.93 ± 0.16	3.81 ± 0.02	−2.44 ± 0.06	2.62	0.008
0.0095	183.10 ± 0.17	2.89 ± 0.02	−2.74 ± 0.07	4.79	0.011
		[BMIM][SCN] + PC + LiCl			
0.0000	178.31 ± 0.32	4.67 ± 0.04	−1.71 ± 0.15		0.015
0.0028	178.98 ± 0.12	−4.92 ± 0.02	21.37 ± 0.05	0.67	0.007
0.0057	179.40 ± 0.08	2.3 ± 0.01	−2.88 ± 0.03	1.09	0.006
0.0100	180.45 ± 0.12	2.55 ± 0.02	−2.79 ± 0.05	2.13	0.008
		[HMIM][SCN] + PC+ LiBr			
0.0000	213.52 ± 0.60	−13.97 ± 0.09	86.42 ± 0.31		0.026
0.0036	214.46 ± 0.08	−0.66 ± 0.01	7.79 ± 0.3	0.94	0.007
0.0064	216.29 ± 0.07	−0.84 ± 0.01	7.08 ± 0.03	2.77	0.007
0.0099	218.46 ± 0.08	0.57 ± 001	3.20 ± 0.02	4.94	0.005
		[HMIM][SCN] + PC+ LiCl			
0.0000	213.52 ± 0.60	−13.97 ± 0.09	86.42 ± 0.31		0.026
0.0036	214.53 ± 0.07	−2.46 ± 0.01	12.52 ± 0.03	1.01	0.005
0.0065	215.47 ± 0.02	0.20 ± 0.00	4.97 ± 0.01	1.95	0.002
0.0104	216.39 ± 0.07	−0.07 ± 0.01	4.18 ± 0.03	2.87	0.006
		[OMIM][SCN] + PC+ LiBr			
0.0000	244.84 ± 0.24	2.44 ± 0.04	90.02 ± 0.15		0.009
0.0038	246.94 ± 0.07	3.09 ± 0.01	−3.07 ± 0.04	2.10	0.005
0.0060	248.58 ± 0.22	−3.86 ± 0.03	21.02 ± 0.12	3.74	0.016
0.0092	249.73 ± 0.14	3.37 ± 0.02	−3.09 ± 0.07	4.89	0.010
		[OMIM][SCN] + PC+ LiCl			
0.0000	244.84 ± 0.24	2.44 ± 0.04	90.02 ± 0.15		0.009
0.0032	246.64 ± 0.16	3.67 ± 0.02	−3.20 ± 0.08	1.80	0.010
0.0060	248.10 ± 0.16	3.60 ± 0.02	−3.16 ± 0.08	3.26	0.010
0.0100	249.73 ± 0.08	3.18 ± 0.01	−3.07 ± 0.04	4.89	0.006

[a]Standard uncertainties for molality, temperature, and pressure were (m) = 0.002 mol kg^{-1}, u (T) = 0.02K, and u (P) = 10 hPa, respectively, with a 0.68 level of confidence.

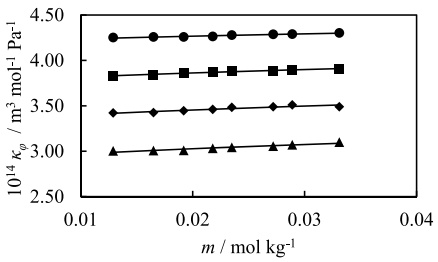

Figure 8. Apparent molar isentropic compressibility κ_φ values of [BMIM][SCN] in PC versus its molality m at different temperatures. (●) T = 288.15 K, (■) T = 298.15 K, (♦) T = 308.15 K, and (▲) T = 318.15 K, and solid lines represent the Redlich−Mayer model.

effect rather than LiCl. Although the addition of the lithium halide salts leads to an increase in the compressibility of the ILs, LiBr has a stronger effect rather than LiCl. To summarize, [OMIM][SCN] is an appropriate cosolvent for Li-ion battery electrolytes that can enhance the mechanical and thermal stability of the batteries.

EXPERIMENTAL SECTION

Chemicals. All of the reagents used in this work are listed in Table 8. Also, the purification methods, supplier company names, and CAS numbers are given. The water content of all components was determined with Karl-Fisher titration (Titrino GPD 751, electrode: Metrohm Pt—6.0338.100).

Ionic Liquids [RMIM][SCN] and their Properties. The ionic liquid synthesis procedure is given in our previous publications with the corresponding density and speed of sound data at different temperatures.[24,26] Also, brief information about the synthesized ionic liquids is given in Table 8.

Apparatus and Procedure. The solutions were prepared using an analytical balance (Shimadzu AW-220) with a precision of ± 1 × 10^{-4} g in a molal-based concentration. The density and speed of sound were measured with a digital densitometer (Anton Paar DSA5000). The instrument was calibrated with air pressure and distilled water. The frequency for the speed of sound measurement was 3 MHz.

ASSOCIATED CONTENT

Supporting Information

The Supporting Information is available free of charge at https://pubs.acs.org/doi/10.1021/acsomega.1c03517.

HNMR spectra of [BMIM][SCN], FT-IR spectra of [BMIM][SCN], HNMR spectra of [HMIM][SCN], FT-IR spectra of [HMIM][SCN], HNMR spectra of [OMIM][SCN], and FT-IR spectra of [OMIM][SCN] (PDF)

https://doi.org/10.1021/acsomega.1c03517
ACS Omega 2021, 6, 27874−27887

Table 6. Partial Molar Isentropic Compressibility κ_{φ}^{0}, Empirical Parameters of eq 17, S_{κ} and B_{κ}, and Standard Deviation of Apparent Molar Isentropic Compressibility $\sigma(\kappa_{\varphi})$ of [RMIM][SCN] in PC T = (288.15−318.15) K under Pressure (P = 0.086 MPa)[a]

T (K)	$10^{14}\,\kappa_{\varphi}^{0}$ (m^3 mol^{-1} Pa^{-1})	$10^{14}\,S_{\kappa}$ (m^3 mol$^{-3/2}$ kg$^{1/2}$ Pa^{-1})	$10^{14}\,B_{\kappa}$ (m^3 mol^{-2} kg Pa^{-1})	$10^{14}\,\sigma\,(\kappa_{\varphi}^{0})$
		[BMIM][SCN]		
288.15	4.17 ± 0.07	0.56 ± 0.01	0.81 ± 0.03	0.004
298.15	3.72 ± 0.07	0.89 ± 0.01	0.91 ± 0.03	0.004
308.15	3.27 ± 0.22	1.14 ± 0.03	0.99 ± 0.10	0.01
318.15	2.84 ± 0.09	1.15 ± 0.01	1.02 ± 0.04	0.009
		[HMIM][SCN]		
288.15	5.55 ± 0.13	1.35 ± 0.02	1.01 ± 0.06	0.046
298.15	5.13 ± 0.31	1.81 ± 0.04	1.15 ± 0.16	0.014
308.15	4.72 ± 0.13	1.93 ± 0.02	1.19 ± 0.06	0.006
318.15	4.43 ± 0.20	1.99 ± 0.03	1.22 ± 0.10	0.010
		[OMIM][SCN]		
288.15	6.12 ± 0.14	−2.83 ± 0.02	57.96 ± 0.09	0.008
298.15	5.83 ± 0.24	−7.97 ± 0.04	81.41 ± 0.15	0.013
308.15	5.51 ± 0.22	−10.83 ± 0.04	92.51 ± 0.14	0.013
318.15	5.02 ± 0.26	−11.47 ± 0.04	94.37 ± 0.16	0.014

[a]Standard uncertainties for temperature and pressure were u (T) = 0.02K and u (P) = 10 hPa, respectively, with a 0.68 level of confidence.

Table 7. Partial Molar Isentropic Compressibility κ_{φ}^{0}, Empirical Parameters of eq 17, S_{κ} and B_{κ}, and Standard Deviation of Apparent Molar Isentropic Compressibility $\sigma(\kappa_{\varphi})$ of [RMIM][SCN] in (PC + LiX) at Different Concentrations of LiX at T = 298.15 K under Pressure (P = 0.086 MPa)[a]

m_{LiX} (mol kg^{-1})	$10^{14}\,\kappa_{\varphi}^{0}$ (m^3 mol^{-1} Pa^{-1})	$10^{14}\,S_{\kappa}$ (m^3 mol$^{-3/2}$ kg$^{1/2}$ Pa^{-1})	$10^{14}\,B_{\kappa}$ (m^3 mol^{-2} kg Pa^{-1})	$10^{14}\,\sigma\,(\kappa_{\varphi}^{0})$
		[BMIM][SCN] + PC + LiBr		
0.0000	3.72 ± 0.07	0.89 ± 0.01	0.91 ± 0.03	0.004
0.0035	5.05 ± 0.15	−3.44 ± 0.02	−0.49 ± 0.06	0.009
0.0056	5.37 ± 0.22	−3.09 ± 0.03	−0.40 ± 0.09	0.011
0.0095	5.76 ± 0.39	−3.03 ± 0.05	−0.38 ± 0.16	0.023
		[BMIM][SCN] + PC + LiCl		
0.0000	3.72 ± 0.07	0.89 ± 0.01	0.91 ± 0.04	0.004
0.0028	4.45 ± 0.05	−1.11 ± 0.01	0.26 ± 0.02	0.006
0.0057	4.71 ± 0.06	−1.11 ± 0.01	0.24 ± 0.02	0.005
0.0100	5.08 ± 0.08	−0.85 ± 0.01	0.32 ± 0.03	0.005
		[HMIM][SCN] + PC+ LiBr		
0.0000	5.13 ± 0.31	1.81 ± 0.04	1.15 ± 0.16	0.014
0.0036	6.80 ± 0.07	−1.20 ± 0.01	0.16 ± 0.03	0.007
0.0064	7.10 ± 0.05	−0.85 ± 0.01	0.29 ± 0.02	0.006
0.0099	7.42 ± 0.03	−0.63 ± 0.00	0.35 ± 0.01	0.003
		[HMIM][SCN] + PC+ LiCl		
0.0000	5.13 ± 0.31	1.81 ± 0.04	1.15 ± 0.16	0.014
0.0036	6.54 ± 0.09	−0.76 ± 0.01	0.33 ± 0.04	0.007
0.0065	6.89 ± 0.06	−0.87 ± 0.01	0.30 ± 0.02	0.008
0.0104	7.33 ± 0.06	−0.90 ± 0.01	0.26 ± 0.03	0.008
		[OMIM][SCN] + PC+ LiBr		
0.0000	5.83 ± 0.24	−7.97 ± 0.04	81.41 ± 0.15	0.013
0.0038	8.59 ± 0.07	−2.17 ± 0.01	−0.03 ± 0.04	0.006
0.0060	8.75 ± 0.09	−1.6 ± 0.01	0.14 ± 0.05	0.011
0.0092	9.05 ± 0.09	−2.14 ± 0.01	−0.03 ± 0.05	0.009
		[OMIM][SCN] + PC+ LiCl		
0.0000	5.83 ± 0.24	−7.97 ± 0.04	81.41 ± 0.15	0.013
0.0032	8.26 ± 0.11	−1.27 ± 0.02	0.20 ± 0.05	0.007
0.0060	8.60 ± 0.04	−1.66 ± 0.01	0.10 ± 0.02	0.006
0.0100	9.12 ± 0.10	−2.16 ± 0.02	−0.04 ± 0.05	0.008

[a]Standard uncertainties for molality, temperature, and pressure were u (m) = 0.002 mol kg^{-1}, u (T) = 0.02K, and u (P) = 10 hPa, respectively, with a 0.68 level of confidence.

https://doi.org/10.1021/acsomega.1c03517
ACS Omega 2021, 6, 27874−27887

Table 8. Summary of the Chemicals and their Characteristics That Were Used in This Work

Chemical name	CAS number	abbreviation	structure	Supplier	Initial mass fraction purity	Purification method	Water content (ppm)	Final mass fraction purity	Analysis method
Lithium bromide	7550-35-8		Li^+ Br^-	Merck	>0.99	Dried at 398.15 K	16		KF
Lithium chloride	7447-41-8		Li^+ Cl^-	Merck	>0.99	Dried at 393.15 K	12		KF
Propylene carbonate	108-32-7	PC	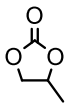	Samchun	>0.995	None	anhydrous		KF
1-butyl-3-methylimidazolium thiocyanate	344790-87-0	[BMIM][SCN]	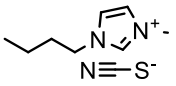	Synthesized		Extraction / filtration / rotary evaporator / vacuum	120	>0.93	H'NMR / FT-IR / KF
1-hexyl-3-methylimidazolium thiocyanate	847499-74-5	[HMIM][SCN]	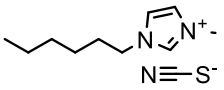	Synthesized		Extraction / filtration / rotary evaporator / vacuum	95	>0.97	H'NMR / FT-IR / KF
1-octyl-3-methylimidazolium thiocyanate	847499-72-3	[OMIM][SCN]	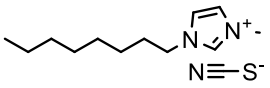	Synthesized		Extraction / filtration / rotary evaporator / vacuum	115	>0.97	H'NMR / FT-IR / KF

AUTHOR INFORMATION

Corresponding Author

Hemayat Shekaari − *Department of Physical Chemistry, University of Tabriz, Tabriz 5166616471, Iran;* orcid.org/0000-0002-5134-6330; Email: hemayatt@yahoo.com

Authors

Behrang Golmohammadi − *Department of Physical Chemistry, University of Tabriz, Tabriz 5166616471, Iran*

Mohammed Taghi Zafarani-Moattar − *Department of Physical Chemistry, University of Tabriz, Tabriz 5166616471, Iran;* orcid.org/0000-0002-2174-1639

Complete contact information is available at: https://pubs.acs.org/10.1021/acsomega.1c03517

Notes

The authors declare no competing financial interest.

ACKNOWLEDGMENTS

The authors wish to thank the financial support from the Graduate Council of the University of Tabriz.

REFERENCES

(1) Holtstiege, F.; Wilken, A.; Winter, M.; Placke, T. Running out of Lithium? A Route to Differentiate between Capacity Losses and Active Lithium Losses in Lithium-Ion Batteries. *Phys. Chem. Chem. Phys.* **2017**, *19*, 25905−25918.

(2) Guo, Z. Y.; Ji, Z. Y.; Chen, H. Y.; Liu, J.; Zhao, Y. Y.; Li, F.; Yuan, J. S. Effect of Impurity Ions in the Electrosorption Lithium Extraction Process: Generation and Restriction of "Selective Concentration Polarization. *ACS Sustainable Chem. Eng.* **2020**, *8*, 11834−11844.

(3) Kazemzadeh, H.; Karimi-Sabet, J.; Towfighi Darian, J.; Adhami, A. Evaluation of Polymer Inclusion Membrane Efficiency in Selective Separation of Lithium Ion from Aqueous Solution. *Sep. Purif. Technol.* **2020**, *251*, No. 117298.

(4) Lee, Y.; Cha, J. H.; Jung, D. Y. Lithium Separation by Growth of Lithium Aluminum Layered Double Hydroxides on Aluminum Metal Substrates. *Solid State Sci.* **2020**, *110*, No. 106488.

(5) Linneen, N.; Bhave, R.; Woerner, D. Purification of Industrial Grade Lithium Chloride for the Recovery of High Purity Battery Grade Lithium Carbonate. *Sep. Purif. Technol.* **2019**, *214*, 168−173.

(6) Lu, H.; Chen, Z.; Yuan, Y.; Du, H.; Wang, J.; Liu, X.; Hou, Z.; Zhang, K.; Fang, J.; Qu, Y. A Rational Balance Design of Hybrid Electrolyte Based on Ionic Liquid and Fluorinated Ether in Lithium Sulfur Batteries. *J. Electrochem. Soc.* **2019**, *166*, A2453−A2458.

(7) Wang, X.; Salari, M.; Jiang, D.; et al. Electrode Material−Ionic Liquid Coupling for Electrochemical Energy Storage. *Nature* **2020**, *5*, 787−808.

(8) Andrea Calderón, C.; Vizintin, A.; Bobnar, J.; Barraco, D. E.; Leiva, E. P. M.; Visintin, A.; Fantini, S.; Fischer, F.; Dominko, R. Lithium Metal Protection by a Cross-Linked Polymer Ionic Liquid and Its Application in Lithium Battery. *ACS Appl. Energy Mater.* **2020**, *3*, 2020−2027.

(9) Yang, C.; Wang, S.; Zhang, X.; Zhang, Q.; Ma, W.; Yu, S.; Sun, G. Substituent Effect of Imidazolium Ionic Liquid: A Potential Strategy for High Coulombic Efficiency Al Battery. *J. Phys. Chem. C* **2019**, *123*, 11522−11528.

(10) Molinari, N.; Mailoa, J. P.; Kozinsky, B. General Trend of a Negative Li Effective Charge in Ionic Liquid Electrolytes. *J. Phys. Chem. Lett.* **2019**, *10*, 2313−2319.

(11) Falcone, R. D.; Correa, N. M.; Silber, J. J. Amphiphilic Ionic Liquids as Sustainable Components to Formulate Promising Vesicles to Be Used in Nanomedicine. In *CurrentOpinion in Green and Sustainable Chemistry*; Elsevier B.V., 2020; p 100382.

(12) Barbosa, L. C.; Nascimento, M. V. da C.; Araújo, O. de Q. F.; de Medeiros, J. L. A Cleaner and More Sustainable Decarbonation Process via Ionic-Liquid Absorption for Natural Gas with High Carbon Dioxide Content. *J. Clean. Prod.* **2020**, *242*, No. 118421.

(13) Francis, C. F. J.; Kyratzis, I. L.; Best, A. S. Lithium-Ion Battery Separators for Ionic-Liquid Electrolytes: A Review. *Adv. Mater.* **2020**, *32*, No. 1904205.

(14) Liu, X.; Zhang, S.; Wang, J.; Wang, J.; Shao, Y.; Zhu, L. Biochemical Responses and DNA Damage in Earthworms (Eisenia

Fetida) Induced by Ionic Liquid [Omim]PF6. *Environ. Sci. Pollut. Res.* **2016**, *23*, 6836−6844.
(15) Deng, X. Y.; Li, D.; Wang, L.; Hu, X. L.; Cheng, J.; Gao, K. Potential Toxicity of Ionic Liquid ([C12mim]BF4) on the Growth and Biochemical Characteristics of a Marine Diatom Phaeodactylum Tricornutum. *Sci. Total Environ.* **2017**, *586*, 675−684.
(16) Li, W.; Zhu, L.; Du, Z.; Li, B.; Wang, J.; Wang, J.; Zhang, C.; Zhu, L. Acute Toxicity, Oxidative Stress and DNA Damage of Three Task-Specific Ionic Liquids ([C2NH2MIm]BF4, [MOEMIm]BF4, and [HOEMIm]BF4) to Zebrafish (Danio Rerio). *Chemosphere* **2020**, *249*, No. 126119.
(17) Rout, A.; Binnemans, K. Efficient Separation of Transition Metals from Rare Earths by an Undiluted Phosphonium Thiocyanate Ionic Liquid. *Phys. Chem. Chem. Phys.* **2016**, *18*, 16039−16045.
(18) Gupta, K. M.; Chen, Y.; Hu, Z.; Jiang, J. Metal-Organic Framework Supported Ionic Liquid Membranes for CO 2 Capture: Anion Effects. *Phys. Chem. Chem. Phys.* **2012**, *14*, 5785−5794.
(19) Nam, J. E.; Jo, H. J.; Kang, J. K.; Woo, S.; Hwang, D. K. Optimization of Electrolyte Components on the Performance of Organic-Dye-Sensitized Solar Cells. *J. Nanosci. Nanotechnol.* **2017**, *17*, 8100−8104.
(20) Rosol, Z. P.; German, N. J.; Gross, S. M. Solubility, Ionic Conductivity and Viscosity of Lithium Salts in Room Temperature Ionic Liquids. *Green Chem.* **2009**, *11*, 1453−1457.
(21) Vogl, T.; Menne, S.; Balducci, A. Mixtures of Protic Ionic Liquids and Propylene Carbonate as Advanced Electrolytes for Lithium-Ion Batteries. *Phys. Chem. Chem. Phys.* **2014**, *16*, 25014−25023.
(22) Levy, N. R.; Lifshits, S.; Yohanan, E.; Ein-Eli, Y. Hybrid Ionic Liquid Propylene Carbonate-Based Electrolytes for Aluminum-Air Batteries. *ACS Appl. Energy Mater* **2020**, *3*, 2585−2592.
(23) Karuppasamy, K.; Vikraman, D.; Hwang, I. T.; Kim, H. J.; Nichelson, A.; Bose, R.; Kim, H. S. Nonaqueous Liquid Electrolytes Based on Novel 1-Ethyl-3-Methylimidazolium Bis (Nonafluorobutane-1-Sulfonyl Imidate) Ionic Liquid for Energy Storage Devices. *J. Mater. Res. Technol.* **2020**, *9*, 1251−1260.
(24) Shekaari, H.; Zafarani-Moattar, M. T.; Golmohammadi, B. Solvation Properties of 1-Alkyl-3-Methylimidazolium Thiocyanate Ionic Liquids in the Presence of Lithium Halide Salts in N-Methyl-2-Pyrrolidone. *J. Mol. Liq.* **2019**, *280*, 191−204.
(25) Zafarani-Moattar, M. T.; Shekaari, H.; Sadrmousavi Dizaj, A. Investigation of Solute-Solvent Interactions in Binary and Quaternary Solutions Containing Lithium Perchlorate, Propylene Carbonate, and the Deep Eutectic Solvent (Choline Chloride/Ethylene Glycol) at T=(288.15 to 318.15) K. *J. Mol. Liq.* **2020**, *319*, No. 114090.
(26) Shekaari, H.; Taghi Zafarani-Moattar, M.; Golmohammadi, B. Thermodynamic and Transport Properties of Ionic Liquids, 1-Alkyl-3-Methylimidazolium Thiocyanate in the Aqueous Lithium Halides Solutions. *J. Chem. Thermodyn.* **2020**, *141*, No. 105953.
(27) Vraneš, M.; Zec, N.; Tot, A.; Papović, S.; Dožić, S.; Gadžurić, S. Density, Electrical Conductivity, Viscosity and Excess Properties of 1-Butyl-3-Methylimidazolium Bis(Trifluoromethylsulfonyl)Imide + Propylene Carbonate Binary Mixtures. *J. Chem. Thermodyn.* **2014**, *68*, 98−108.
(28) Tyunina, E.; Afanas'ev, V.; Chekunova, M. Viscosity and Density of Solutions of Tetraethylammonium Tetrafluoroborate in Propylene Carbonate at Different Temperatures. *J. Solution Chem.* **2012**, *41*, 307−317.
(29) Moumouzias, G.; Ritzoulis, G. Relative Permittivities and Refractive Indices of Propylene Carbonate + Toluene Mixtures from 283.15 K to 313.15 K. *J. Chem. Eng. Data* **1997**, *42*, 710−713.
(30) Zhao, Y.; Wang, J.; Xuan, X.; Lu, J. Effect of Temperature on Excess Molar Volumes and Viscosities for Propylene Carbonate + N,N-Dimethylformamide Mixtures. *J. Chem. Eng. Data* **2000**, *45*, 440−444.
(31) Murrieta-Guevara, F.; Trejo Rodríguez, A. Liquid Density as a Function of Temperature of Five Organic Solvents. *J. Chem. Eng. Data* **1984**, *29*, 204−206.
(32) Wang, H.; Hu, L.; Wu, Y. Excess Volumes and Partial Molar Volumes of Binary Mixtures of 1,2-Propanediol Carbonate with Xylene in the Temperature Range of (293.15 to 353.15) K. *J. Chem. Thermodyn.* **2005**, *37*, 1119−1129.
(33) Pires, J.; Timperman, L.; Jacquemin, J.; Balducci, A.; Anouti, M. Density, Conductivity, Viscosity, and Excess Properties of (Pyrrolidinium Nitrate-Based Protic Ionic Liquid + Propylene Carbonate) Binary Mixture. *J. Chem. Thermodyn.* **2013**, *59*, 10−19.
(34) Barthel, J.; Neueder, R.; Roch, H. Density, Relative Permittivity, and Viscosity of Propylene Carbonate+dimethoxyethane Mixtures from 25 °C to 125 °C. *J. Chem. Eng. Data* **2000**, *45*, 1007−1011.
(35) Zhao, Y. H.; Abraham, M. H.; Zissimos, A. M. Fast Calculation of van Der Waals Volume as a Sum of Atomic and Bond Contributions and Its Application to Drug Compounds. *J. Org. Chem.* **2003**, *68*, 7368−7373.
(36) Bondi, A. Van Der Waals Volumes and Radii. *J. Phys. Chem. A.* **1964**, *68*, 441−451.
(37) Chernyak, Y.; Clements, J. H. Vapor Pressure and Liquid Heat Capacity of Alkylene Carbonates. *J. Chem. Eng. Data* **2004**, *49*, 1180−1184.
(38) Piekarski, H.; Kubalczyk, K.; Wasiak, M. Volumes, Heat Capacities, and Compressibilities of the Mixtures of Acetonitrile with N, N -Dimethylacetamide and Propylene Carbonate. *J. Chem. Eng. Data* **2010**, *55*, 5435−5440.
(39) Hepler, L. G. Thermal Expansion and Structure in Water and Aqueous Solutions. *Can. J. Chem* **1969**, *47*, 4613−4617.
(40) Gorobets, M. I.; Ataev, M. B.; Gafurov, M. M.; Kirillov, S. A. Speciation in Solutions of Lithium Salts in Dimethyl Sulfoxide, Propylene Carbonate, and Dimethyl Carbonate from Raman Data: A Minireview. *J. Spectrosc.* **2016**, *2016*, No. 6978560.
(41) Angenendt, K.; Johansson, P. Ionic Liquid Based Lithium Battery Electrolytes: Charge Carriers and Interactions Derived by Density Functional Theory Calculations. *J. Phys. Chem. B* **2011**, *115*, 7808−7813.
(42) Hinton, J. F.; Amis, E. S. Solvation Numbers of Ions. *Chem. Rev.* **1971**, *71*, 627−674.

https://doi.org/10.1021/acsomega.1c03517
ACS Omega 2021, 6, 27874−27887